

Modification of 1,2,4,5-tetrazine with cationic rhenium(I) polypyridine units to afford phosphorogenic bioorthogonal probes with enhanced reaction kinetics

Alex Wing-Tat Choi, Karson Ka-Shun Tso, Vicki Man-Wai Yim, Hua-Wei Liu and
Kenneth Kam-Wing Lo*

*Department of Biology and Chemistry, City University of Hong Kong, Tat Chee
Avenue, Kowloon, Hong Kong, P. R. China*

Electronic Supplementary Information

EXPERIMENTAL SECTION

Materials and synthesis. All solvents were of analytical reagent grade and purified according to standard procedures.¹ Zinc trifluoromethanesulfonate, 3-cyanopyridine, 4-cyanopyridine, hydrazine monohydrate, sodium nitrite, 2,9-dimethyl-1,10-phenanthroline (Me₂-phen), 4,7-diphenyl-1,10-phenanthroline (Ph₂-phen) and Re₂(CO)₁₀ were purchased from Acros. The dienophiles 5-norbornen-2-ol (NBO) and (1*R*,8*S*,9*S*)-bicyclo[6.1.0]non-4-yn-9-ylmethanol (BCN) were obtained from Aldrich. The labelling reagent (1*R*,8*S*,9*S*)-bicyclo[6.1.0]non-4-yn-9-ylmethyl-*N*-succinimidyl carbonate (BCN-NHS) was purchased from Barry & Associates, Inc. Bovine serum albumin (BSA), human serum albumin (HSA) and apo-transferrin (aTf) were obtained from Calbiochem. MTT was obtained from Sigma. All these chemicals were used without further purification. [Re(N^N)(CO)₃(CH₃CN)](CF₃SO₃) was prepared as described previously.² All buffer components were of biological grade and used as received. Autoclaved Milli-Q water was used for the preparation of aqueous solutions. HeLa cells were obtained from American Type Culture Collection. Dulbecco's modified Eagle's medium (DMEM), fetal bovine serum (FBS), phosphate buffered saline (PBS), trypsin-EDTA, Novex[®] sharp pre-stained protein standard and penicillin/streptomycin were purchased from Invitrogen. The growth medium for cell culture contained DMEM with 10% FBS and 1% penicillin/streptomycin.

6-Methyl-3-pyridin-3-yl-1,2,4,5-tetrazine (py-3-Tz). A mixture of 3-cyanopyridine (400 mg, 3.8 mmol), CH₃CN (2.00 mL, 38.3 mmol), zinc trifluoromethanesulfonate (349 mg, 1.0 mmol) and hydrazine monohydrate (4.66 mL, 95.0 mmol) was heated in an oil bath at 70°C under an inert atmosphere of nitrogen for 48 h. After the mixture was cooled to room temperature, sodium nitrite (5.2 g, 76.0 mmol) in 5 mL H₂O was added and followed by 1 M HCl until pH = 3. The

aqueous phase was extracted with CH₂Cl₂ (100 mL × 3). The combined organic layer was dried over MgSO₄ and evaporated to dryness yielding a red solid, which was purified by column chromatography on silica gel. The desired product was eluted with *n*-hexane/ethyl acetate (4:1, *v/v*). The solvent was removed under vacuum to afford the product as a purple solid. Yield: 101.0 mg (15%). ¹H NMR (400 MHz, CDCl₃, 298 K): δ 9.71 (s, 1H, H2 of pyridine), 8.88 – 8.84 (m, 2H, H4 and H6 of pyridine), 7.55 (t, 1H, *J* = 8.0 Hz, H5 of pyridine), 3.15 (s, 3H, CH₃). Positive-ion ESI-MS ion clusters at *m/z* 174 {M + H⁺}⁺.

6-Methyl-3-pyridin-4-yl-1,2,4,5-tetrazine (py-4-Tz). The synthetic procedure was similar to that for the preparation of py-3-Tz, except that 4-cyanopyridine was used instead of 3-cyanopyridine. Yield: 118.8 mg (18%). ¹H NMR (400 MHz, CDCl₃, 298 K): δ 8.91 (d, 2H, *J* = 6.0 Hz, H2 and H6 of pyridine), 8.45 (d, 2H, *J* = 6.4 Hz, H3 and H5 of pyridine), 3.17 (s, 3H, CH₃). Positive-ion ESI-MS ion clusters at *m/z* 174 {M + H⁺}⁺.

3,6-Bis(pyridin-3-yl)-1,2,4,5-tetrazine (py-Tz-py). The synthetic procedure was similar to that for the preparation of py-3-Tz, except that the amount of 3-cyanopyridine was increased from 400 mg to 800 mg and no CH₃CN was used. Yield: 198.0 mg (22%). ¹H NMR (400 MHz, CDCl₃, 298 K): δ 9.88 (s, 2H, H2 of pyridine), 8.94 – 8.91 (m, 4H, H4 and H6 of pyridine), 7.60 (t, 2H, *J* = 6.4 Hz, H5 of pyridine). Positive-ion ESI-MS ion clusters at *m/z* 237 {M + H⁺}⁺.

[Re(N[^]N)(CO)₃(py-3-Tz)](CF₃SO₃) (N[^]N = Me₂-phen (1a), Ph₂-phen (2a)). A mixture of [Re(N[^]N)(CO)₃(CH₃CN)](CF₃SO₃) (0.19 mmol) and py-3-Tz (0.19 mmol) in THF (30 mL) was refluxed under an inert atmosphere of nitrogen for 12 h. The mixture was evaporated to dryness to afford a red solid, which was purified by column chromatography on silica gel. The desired product was eluted with a mixture

of CH₂Cl₂ and MeOH. Recrystallisation of the product from CH₂Cl₂/diethyl ether afforded the tetrazine complex as red crystals. Complex **1a**. Yield: 78 mg (51%). ¹H NMR (400 MHz, CD₃OD, 298 K): δ 8.81 – 8.78 (m, 2H, H2 and H6 of pyridine), 8.69 (d, 2H, *J* = 8.4 Hz, H4 and H7 of Me₂-Phen), 8.29 (d, 1H, *J* = 5.2 Hz, H4 of pyridine), 8.18 (d, 2H, *J* = 6.3 Hz, H3 and H8 of Me₂-phen), 7.99 (s, 2H, H5 and H6 of Me₂-phen), 7.46 – 7.42 (m, 1H, H5 of pyridine), 3.50 (s, 6H, CH₃ at C2 and C9 of Me₂-phen), 3.04 (s, 3H, CH₃ of py-3-Tz). IR (KBr) ν /cm⁻¹: 2030 (s, C≡O), 1918 (s, C≡O), 1150 (m, CF₃SO₃⁻), 1032 (m, CF₃SO₃⁻). Positive-ion ESI-MS ion cluster at *m/z* 651 {M – CF₃SO₃⁻}⁺. Anal. Calcd for ReC₂₆H₁₉N₇O₆SF₃·0.5H₂O: C, 38.57; H, 2.49; N, 12.11. Found: C, 38.51; H, 2.89; N, 12.29. Complex **2a**. Yield: 73 mg (42%). ¹H NMR (400 MHz, CD₃OD, 298 K): δ 9.85 (d, 2H, *J* = 5.2 Hz, H2 and H9 of Ph₂-phen), 9.30 (s, 1H, H2 of pyridine), 8.92 – 8.91 (m, 2H, H4 and H6 of pyridine), 8.20 – 8.19 (m, 4H, H3, H5, H6 and H8 of Ph₂-phen), 7.71 – 7.64 (m, 11H, H5 of pyridine and C₆H₅ at C4 and C7 of Ph₂-phen), 3.04 (s, 3H, CH₃ of py-3-Tz). IR (KBr) ν /cm⁻¹: 2032 (s, C≡O), 1917 (s, C≡O), 1152 (m, CF₃SO₃⁻), 1031 (m, CF₃SO₃⁻). Positive-ion ESI-MS ion cluster at *m/z* 776 {M – CF₃SO₃⁻}⁺. Anal. Calcd for ReC₃₆H₂₃N₇O₆SF₃·2H₂O·0.5(CH₃CH₂)₂O: C, 45.73; H, 3.23; N, 9.82. Found: C, 45.70; H, 3.08; N, 9.69.

[Re(N[^]N)(CO)₃(py-4-Tz)](CF₃SO₃) (N[^]N = Me₂-phen (1b**), Ph₂-phen (**2b**)).**

The synthetic procedure was similar to that for the preparation of [Re(N[^]N)(CO)₃(py-3-Tz)](CF₃SO₃), except that py-4-Tz was used instead of py-3-Tz. Complex **1b**. Yield: 65 mg (43%). ¹H NMR (400 MHz, CD₃OD, 298 K): 8.70 (d, 2H, *J* = 8.4 Hz, H4 and H7 of Me₂-phen), 8.23 – 8.22 (m, 4H, H2, H3, H5 and H6 of pyridine), 8.16 (d, 2H, *J* = 8.4 Hz, H3 and H8 of Me₂-phen), 7.80 (s, 2H, H5 and H6 of Me₂-phen),

3.49 (s, 6H, CH₃ at C2 and C9 of Me₂-phen), 3.04 (s, 3H, CH₃ of py-4-Tz). IR (KBr) ν/cm^{-1} : 2025 (s, C≡O), 1902 (s, C≡O), 1149 (m, CF₃SO₃⁻), 1029 (m, CF₃SO₃⁻). Positive-ion ESI-MS ion cluster at m/z 651 {M – CF₃SO₃⁻}⁺. Anal. Calcd for ReC₂₆H₁₉N₇O₆SF₃·0.5H₂O: C, 38.57; H, 2.49; N, 12.11. Found: C, 38.43; H, 2.85; N, 12.30. Complex **2b**. Yield: 102 mg (58%). ¹H NMR (400 MHz, CD₃OD, 298 K): δ 9.84 (d, 2H, J = 5.6 Hz, H2 and H9 of Ph₂-phen), 8.86 (d, 2H, J = 6.8 Hz, H2 and H6 of pyridine), 8.41 (d, 2H, J = 6.8 Hz, H3 and H5 of pyridine), 8.20 – 8.19 (m, 4H, H3, H5, H6 and H8 of Ph₂-phen), 7.72 – 7.65 (m, 10H, C₆H₅ at C4 and C7 of Ph₂-phen), 3.04 (s, 3H, CH₃ of py-4-Tz). IR (KBr) ν/cm^{-1} : 2032 (s, C≡O), 1918 (s, C≡O), 1154 (m, CF₃SO₃⁻), 1031 (m, CF₃SO₃⁻). Positive-ion ESI-MS ion cluster at m/z 776 {M – CF₃SO₃⁻}⁺. Anal. Calcd for ReC₃₆H₂₃N₇O₆SF₃·H₂O: C, 45.86; H, 2.67; N, 10.40. Found: C, 46.19; H, 3.06; N, 10.08.

[{Re(N[^]N)(CO)₃}₂(μ -py-Tz-py)](CF₃SO₃)₂ (N[^]N = Me₂-phen (1c**), Ph₂-phen (**2c**)).** A mixture of [Re(N[^]N)(CO)₃(CH₃CN)](CF₃SO₃) (0.22 mmol) and py-Tz-py (0.09 mmol) in THF (30 mL) was refluxed under an inert atmosphere of nitrogen for 12 h. The mixture was evaporated to dryness to afford a red solid, which was purified by column chromatography on silica gel. The desired product was eluted with a mixture of CH₂Cl₂ and MeOH. Recrystallisation of the product from CH₂Cl₂/diethyl ether afforded the tetrazine complex as red crystals. Complex **1c**. Yield: 56 mg (40%). ¹H NMR (400 MHz, CD₃OD, 298 K): δ 8.85 (d, 4H, J = 8.0 Hz, H4 and H7 of Me₂-phen), 8.77 – 8.74 (m, 4H, H2 and H6 of pyridine), 8.34 (d, 2H, J = 5.6 Hz, H4 of pyridine), 8.28 (d, 4H, J = 8.4 Hz, H3 and H8 of Me₂-phen), 8.12 (s, 4H, H5 and H6 of Me₂-phen), 7.53 (t, 2H, J = 6.8 Hz, H5 of pyridine), 3.40 (s, 12H, CH₃ at C2 and C9 of Me₂-phen). IR (KBr) ν/cm^{-1} : 2030 (s, C≡O), 1906 (s, C≡O),

1159 (m, CF₃SO₃⁻), 1030 (m, CF₃SO₃⁻). Positive-ion ESI-MS ion cluster at *m/z* 1342 {M – CF₃SO₃⁻}⁺. Anal. Calcd for Re₂C₄₈H₃₂N₁₀O₁₂S₂F₆·2H₂O: C, 37.75; H, 2.38; N, 9.17. Found: C, 37.54; H, 2.72; N, 9.55. Complex **2c**. Yield: 48 mg (30%). ¹H NMR (400 MHz, CD₃OD, 298 K): δ 9.83 (d, 4H, *J* = 5.2 Hz, H2 and H9 of Ph₂-phen), 9.42 (s, 2H, H2 of pyridine), 8.96 (d, 2H, *J* = 8.0 Hz, H6 of pyridine), 8.86 (d, 2H, *J* = 5.6 Hz, H4 of pyridine), 8.18 – 8.16 (m, 8H, H3, H5, H6 and H8 of Ph₂-phen), 7.70 – 7.65 (m, 22H, H5 of pyridine and C₆H₅ at C4 and C7 of Ph₂-phen). IR (KBr) ν/cm⁻¹: 2033 (s, C≡O), 1916 (s, C≡O), 1152 (m, CF₃SO₃⁻), 1030 (m, CF₃SO₃⁻). Positive-ion ESI-MS ion cluster at *m/z* 1591 {M – CF₃SO₃⁻}⁺. Anal. Calcd for Re₂C₆₈H₄₀N₁₀O₁₂S₂F₆·2H₂O: C, 46.00; H, 2.50; N, 7.89. Found: C, 45.88; H, 2.86; N, 8.25.

Instrumentation and methods. ¹H NMR spectra were recorded on a Bruker 400 MHz NMR spectrometer at 298 K. Positive-ion ESI-mass spectra were recorded on a Perkin-Elmer Sciex API 365 mass spectrometer. IR spectra were recorded on a Perkin-Elmer 1600 series FT-IR spectrophotometer. Elemental analyses were carried out on a Vario EL III CHN elemental analyser. Electronic absorption and steady-state emission spectra were recorded on a Hewlett-Packard 8453 diode array spectrophotometer and a SPEX FluoroLog 3-TCSPC spectrophotometer equipped with a Hamamatsu R928 PMT detector, respectively. Emission lifetimes were measured in the Fast MCS lifetime mode with a NanoLED N-375 as the excitation source. All the solutions for photophysical studies were degassed with at least four successive freeze-pump-thaw cycles and stored in a 10-cm³ round-bottomed flask equipped with a sidearm 1-cm fluorescence cuvette and sealed from the atmosphere by a Rotaflo HP6/6 quick-release Teflon stopper. Luminescence quantum yields were measured by the optically dilute method³ using a degassed CH₃CN solution of

[Re(phen)(CO)₃(pyridine)](CF₃SO₃) ($\Phi_{\text{em}} = 0.18$, $\lambda_{\text{ex}} = 355$ nm) as the standard solution.⁴ Details on the SDS-PAGE analysis,⁵ 3-(4,5-dimethylthiazol-2-yl)-2,5-diphenyltetrazolium bromide (MTT) assays,⁶ and inductively coupled plasma-mass spectrometry (ICP-MS)⁶ have been reported previously.

Reactions of the tetrazine complexes and ligands with NBO and BCN. To a solution of the tetrazine complexes and ligands (0.2 μmol) in 10 mL methanol/water (1:1, v/v) was added NBO (22.0 mg, 0.2 mmol) or BCN (0.60 mg, 4.0 μmol) dissolved in 10 mL methanol/water (1:1, v/v). The mixture was stirred in the dark for 3 h at 298 K and the solution was analysed by ESI-MS.

Determination of kinetic rate constants. The second-order rate constants (k_2) of the tetrazine compounds were measured under pseudo first order conditions with a 1000- to 2500-fold excess of NBO or 10- to 25-fold excess of BCN in methanol/water (1:1, v/v). The reaction process was followed by monitoring the exponential decay of the absorbance at ca. 260 or 290 nm. Stock solutions of NBO (20, 30, 40 and 50 mM) and BCN (200, 300, 400 and 500 μM) in methanol/water (1:1, v/v) were prepared. The changes of UV absorbance of the tetrazine compounds (20 μM) in methanol/water (1:1, v/v) were measured immediately after the addition of an equal volume of the prepared dienophile solutions. The final concentrations of the tetrazine compounds were 10 μM and those of the NBO and BCN ranged from 10 to 25 mM and 100 to 250 μM , respectively. Data were fitted to a single-exponential equation to give the observed rate constants, which were then plotted against the concentrations of the dienophiles to obtain the k_2 from the slopes of the plots.

Modification of BSA, HSA and aTf with BCN-NHS. BCN-NHS (0.9 mg, 3.0 μmol) in anhydrous DMSO (50 μL) was added to the protein (BSA, HSA, aTf) (0.3 μmol) in 50 mM carbonate buffer (450 μL) at pH 10. The mixture was stirred for

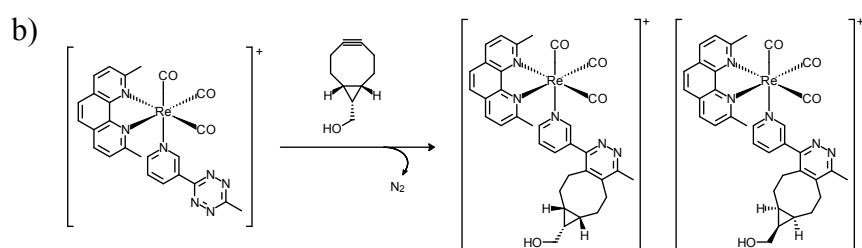
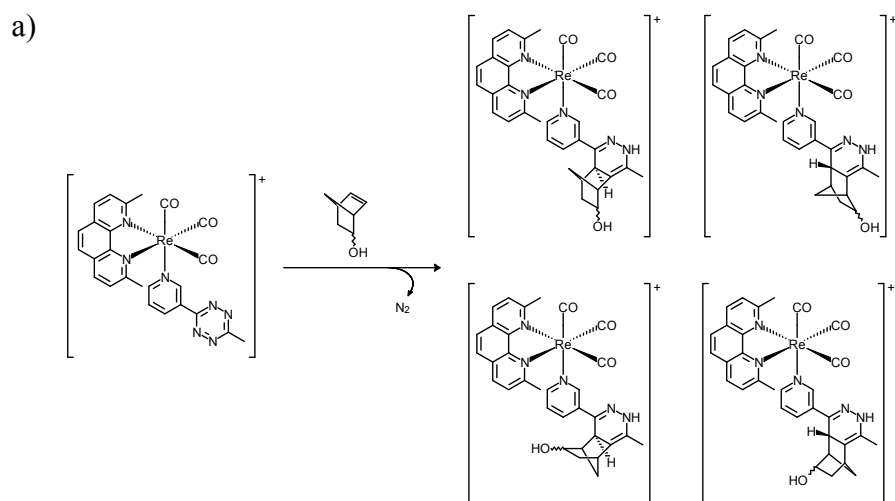
12 h in the dark at 298 K. The precipitate was removed by centrifugation. The filtrate was loaded onto a PD-10 column equilibrated with the same buffer. Volume fractions between 2.5 and 5.0 mL were collected. Then, the BCN-modified protein (BSA-BCN, HSA-BCN, aTf-BCN) was washed successively with potassium phosphate buffer using an YM-50 centricon, and the solution was concentrated to 1.0 mL and stored at 4°C. The proteins were characterized by MALDI-TOF-MS.

Labelling of BCN-modified proteins with the tetrazine complexes. The tetrazine complex (25 nmol) in anhydrous DMSO (50 μ L) was added to the BCN-modified protein (BSA-BCN, HSA-BCN, aTf-BCN) (3.7 nmol) in 50 mM potassium phosphate buffer pH 7.4 (450 μ L). The mixture was stirred for 1 h in the dark at 298 K. Then, an aliquot (10 μ L) of the reaction mixture was analysed by SDS-PAGE. The rhenium-labelled bioconjugates were also characterized by MALDI-TOF-MS, except the aTf conjugate where the signals were extremely weak in the mass spectra.

Live-cell confocal microscopy and bioorthogonal imaging in HeLa cells. HeLa cells in growth medium were seeded on a sterilised coverslip in a 60-mm tissue culture dish and grown at 37°C under a 5% CO₂ atmosphere for 48 h. The culture medium was then removed and replaced with medium/DMSO (99:1, v/v) containing complex **2c** (5 μ M). After incubation for 1 h, the medium was removed and the cell layer was washed gently with PBS (1 mL \times 3). The coverslip was mounted onto a sterilised glass slide and then imaged using a Leica TCS SPE confocal microscope. In the protein imaging experiments, the cells were first treated with BSA-BCN (7.4 μ M) in medium for 30 min. After the incubation, the medium was removed and the cell layer was washed gently with PBS (1 mL \times 3). The cells were then treated with complex **2c** (5 μ M) in medium/DMSO (99:1, v/v) for 30 min and finally washed with PBS (1 mL \times 3). The coverslip was mounted onto a sterilised glass slide and then

imaged using a Leica TCS SPE confocal microscope. The control experiment was performed using the same procedure except that BSA-BCN (7.4 μM) was replaced with unmodified BSA (7.4 μM).

Scheme S1 The bioorthogonal reactions of the tetrazine complex **1a** with the dienophiles (a) NBO and (b) BCN, showing possible dihydropyridazine and pyridazine products, respectively.



Scheme S2 The bioorthogonal labelling of biomolecules using the tetrazine–BCN reaction couple.

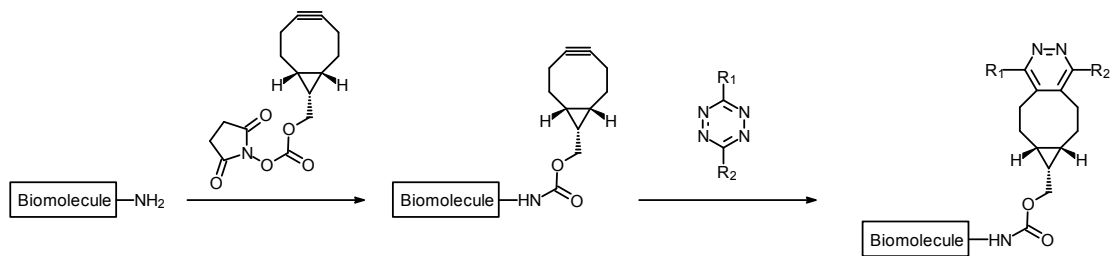


Table S1. Electronic absorption spectral data of the tetrazine complexes at 298 K.

Complex	Solvent	$\lambda_{\text{abs}}/\text{nm}$ ($\epsilon/\text{dm}^3 \text{ mol}^{-1} \text{ cm}^{-1}$)
1a	CH ₂ Cl ₂	280 sh (32 835), 306 sh (21 135), 381 sh (3515), 547 (610)
	CH ₃ CN	284 (30 580), 305 sh (19 500), 371 sh (3220), 535 (525)
1b	CH ₂ Cl ₂	284 (33 320), 305 sh (22 255), 371 sh (6475), 535 (680)
	CH ₃ CN	284 (34 605), 305 sh (24 770), 371 sh (6170), 535 (495)
1c	CH ₂ Cl ₂	284 (58 080), 381 sh (6785), 513 (520)
	CH ₃ CN	284 (47 235), 372 sh (6860), 513 (515)
2a	CH ₂ Cl ₂	264 (40 670), 293 (47 205), 339 sh (20 775), 390 sh (9670), 544 (590)
	CH ₃ CN	260 (50 675), 291 (60 050), 327 sh (24 920), 381 sh (10 585), 533 (515)
2b	CH ₂ Cl ₂	293 (45 580), 339 sh (24 070), 385 sh (10 790), 538 (520)
	CH ₃ CN	291 (52 140), 322 sh (24 570), 381 sh (10 260), 533 (485)
2c	CH ₂ Cl ₂	291 (91 350), 336 sh (34 720), 383 sh (16 165), 533 (485)
	CH ₃ CN	291 (105 435), 332 sh (35 700), 381 sh (15 095), 533 (445)

Table S2. ESI-mass spectrometry data for the tetrazine complexes and ligands after reaction with NBO in methanol/water (1:1, v/v) at 25°C.^a

Compound	Formula for	Mass calculated for	Mass found for
	[M – CF ₃ SO ₃ ⁻] ⁺ or [M + H ⁺] ⁺	[M – CF ₃ SO ₃ ⁻] ⁺ or [M + H ⁺] ⁺	[M – CF ₃ SO ₃ ⁻] ⁺ or [M + H ⁺] ⁺
1a	ReC ₃₂ H ₂₉ N ₅ O ₄ ⁺	734.2	734.7
1b	ReC ₃₂ H ₂₉ N ₅ O ₄ ⁺	734.2	734.6
1c	Re ₂ C ₅₄ H ₄₂ N ₈ O ₁₀ SF ₃ ⁺	1423.2	1423.5
2a	ReC ₄₂ H ₃₃ N ₅ O ₄ ⁺	858.2	858.6
2b	ReC ₄₂ H ₃₃ N ₅ O ₄ ⁺	858.2	858.4
2c	Re ₂ C ₇₄ H ₅₀ N ₈ O ₁₀ SF ₃ ⁺	1671.2	1672.0
Py-3-Tz	C ₁₅ H ₁₈ N ₃ O	256.1	256.6
Py-4-Tz	C ₁₅ H ₁₈ N ₃ O	256.1	256.5
Py-Tz-py	C ₁₉ H ₁₉ N ₄ O	319.2	319.5

^a Additional peaks were detected in the ESI-mass spectra. However, those peaks were due to fragmented products and solvent adducts present in the gaseous phase under our ESI-MS experimental conditions. We do not have evidence that species other than the stereoisomeric dihydropyridazine products were present in the reaction mixtures.

Table S3. ESI-mass spectrometry data for the tetrazine complexes and ligands after reaction with BCN in methanol/water (1:1, v/v) at 25°C.^a

Compound	Formula for	Mass calculated for	Mass found for
	$[M - CF_3SO_3^-]^+$ or $[M + H^+]^+$	$[M - CF_3SO_3^-]^+$ or $[M + H^+]^+$	$[M - CF_3SO_3^-]^+$ or $[M + H^+]^+$
1a	$ReC_{35}H_{33}N_5O_4^+$	774.2	774.2
1b	$ReC_{35}H_{33}N_5O_4^+$	774.2	774.7
1c	$Re_2C_{57}H_{46}N_8O_{10}SF_3^+$	1463.2	1463.1
2a	$ReC_{45}H_{37}N_5O_4^+$	898.2	898.7
2b	$ReC_{45}H_{37}N_5O_4^+$	898.2	898.1
2c	$Re_2C_{77}H_{54}N_8O_{10}SF_3^+$	1711.3	1712.0
Py-3-Tz	$C_{18}H_{22}N_3O$	296.2	296.6
Py-4-Tz	$C_{18}H_{22}N_3O$	296.2	296.6
Py-Tz-py	$C_{22}H_{23}N_4O$	359.2	359.5

^a Additional peaks were detected in the ESI-mass spectra. However, those peaks were due to fragmented products and Na^+ /solvent adducts present in the gaseous phase under our ESI-MS experimental conditions. We do not have evidence that species other than the stereoisomeric pyridazine products were present in the reaction mixtures.

Table S4. BCN-to-protein (*BCN/P*) ratios of the protein-BCN conjugates.

Conjugate	<i>BCN/P</i> ratio
BSA-BCN	5.04 ± 1.24
HSA-BCN	4.08 ± 2.13
aTf-BCN	6.10 ± 1.56

Table S5. Rhenium-to-protein (*Re/P*) ratios of the rhenium-labelled bioconjugates.

Conjugate	<i>Re/P</i> ratio
BSA-1a	1.45 ± 0.82
BSA-1b	1.35 ± 0.23
BSA-1c	2.05 ± 1.32
BSA-2a	1.38 ± 0.26
BSA-2b	1.58 ± 0.38
BSA-2c	1.02 ± 0.65
HSA-2c	0.88 ± 0.33
aTf-2c	<i>a</i>

^a The *Re/P* ratio of the aTf-2c conjugate could not be determined accurately due to extremely weak signals in the MALDI-TOF-mass spectrum.

Table S6. Emission enhancement factors (I/I_0) for the tetrazine complexes (10 μM) upon reaction with BSA-BCN (7.4 μM) in 50 mM potassium phosphate buffer pH 7.4/DMSO (99:1, v/v) at 25°C.

Complex	I/I_0^a
1a	53.7
1b	77.2
1c	18.0
2a	14.2
2b	6.7
2c	17.5

^a I_0 and I are the emission intensities of the tetrazine complexes (10 μM) in the presence of 7.4 μM of unmodified BSA and BSA-BCN, respectively; incubation time = 1 h. These emission enhancement factors are about 19 to 91% of the expected values obtained from the reactions with BCN in aqueous methanol. The lower values may be due to incomplete reactions and the fact that different solvents were used (50% aqueous methanol vs potassium phosphate buffer), as well as the heterogeneous microenvironments of the complexes on the protein surface.

Table S7. Cellular uptake of the tetrazine complexes by HeLa cells.

Complex	No. of mole/fmol ^a
1a	1.27
1b	0.36
1c	2.81
2a	5.20
2b	2.85
2c	3.11

^a Number of moles of rhenium associated with a typical HeLa cell upon incubation with the tetrazine complexes (10 μ M) at 37°C for 1 h.

Fig. S1 ESI-mass spectrum of a mixture of complex **1a** (10 μM) and NBO (10 mM) in methanol/water (1:1, v/v) at 298 K.

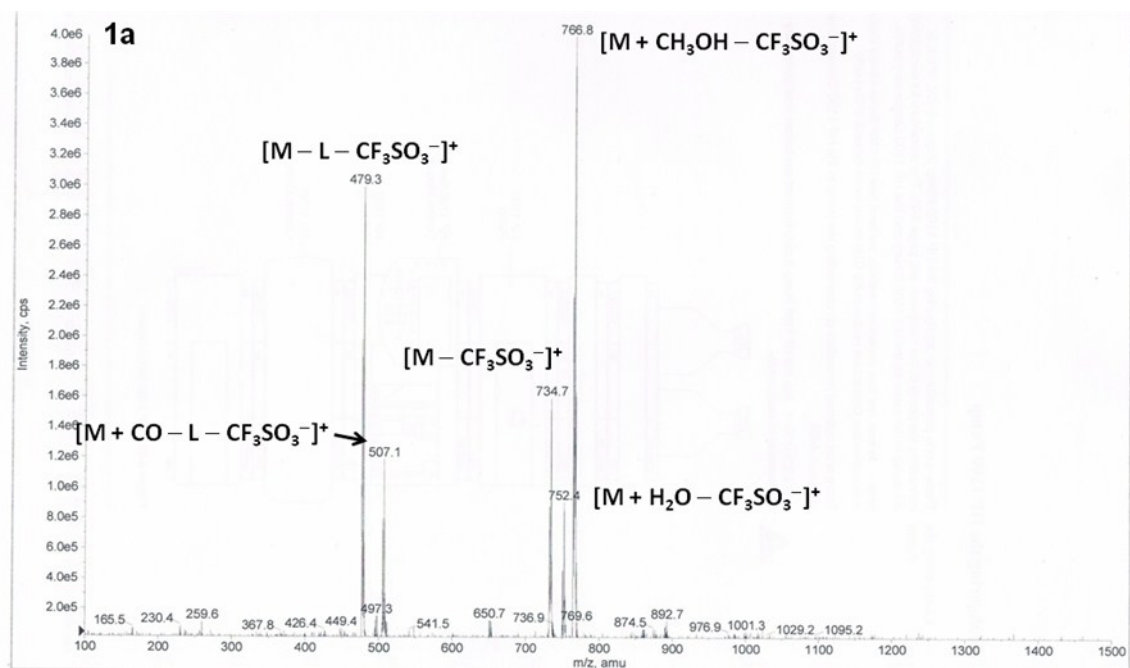


Fig. S2 ESI-mass spectrum of a mixture of complex **1b** (10 μ M) and NBO (10 mM) in methanol/water (1:1, v/v) at 298 K.

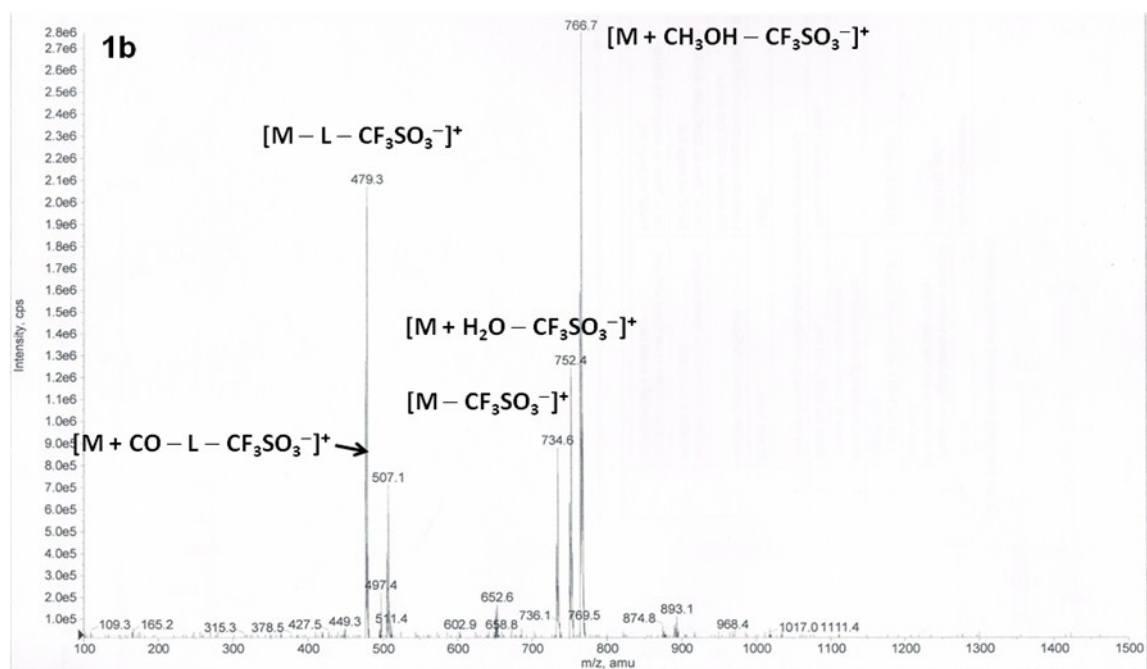


Fig. S3 ESI-mass spectrum of a mixture of complex **1c** (10 μ M) and NBO (10 mM) in methanol/water (1:1, v/v) at 298 K.

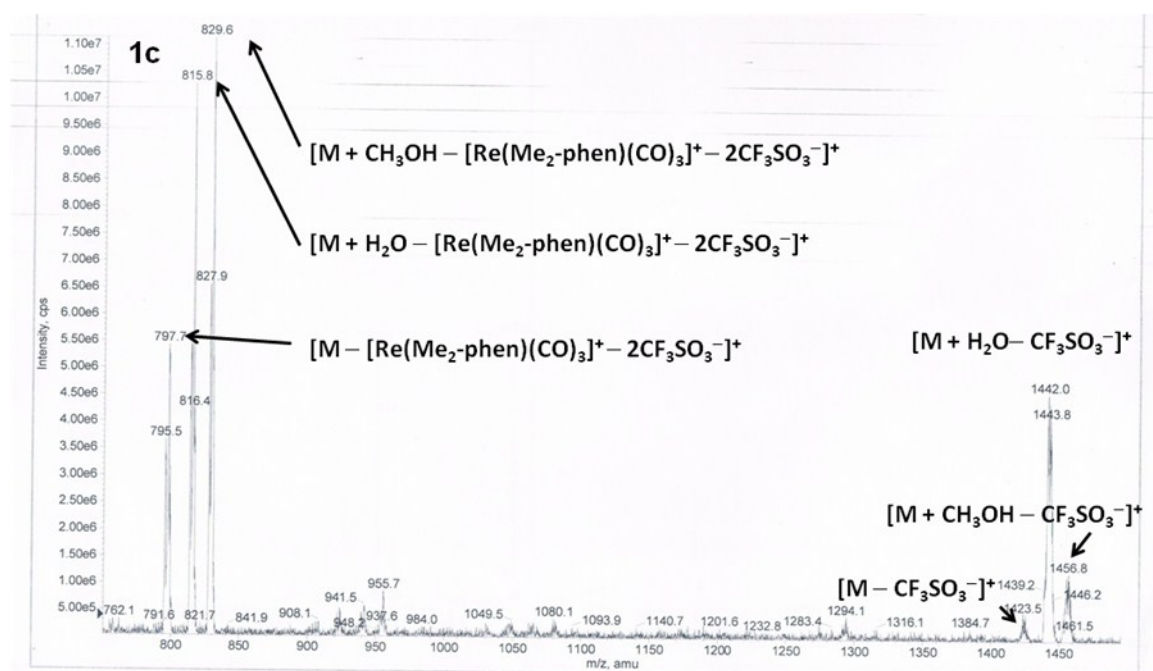


Fig. S4 ESI-mass spectrum of a mixture of complex **2a** (10 μ M) and NBO (10 mM) in methanol/water (1:1, v/v) at 298 K.

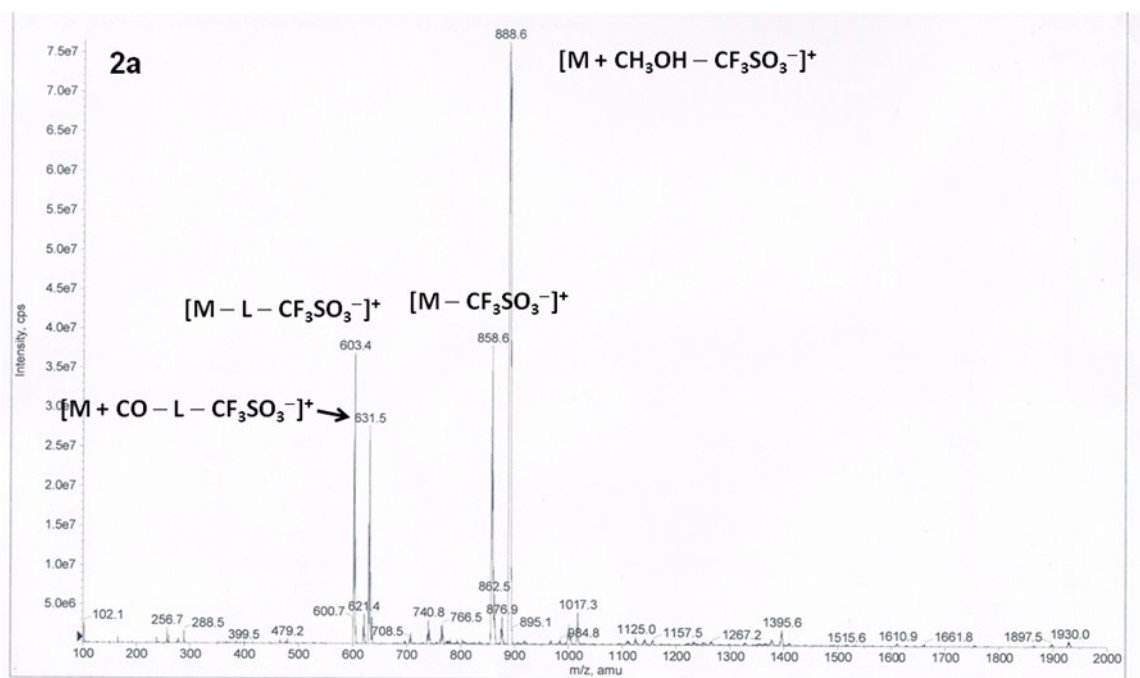


Fig. S5 ESI-mass spectrum of a mixture of complex **2b** (10 μ M) and NBO (10 mM) in methanol/water (1:1, v/v) at 298 K.

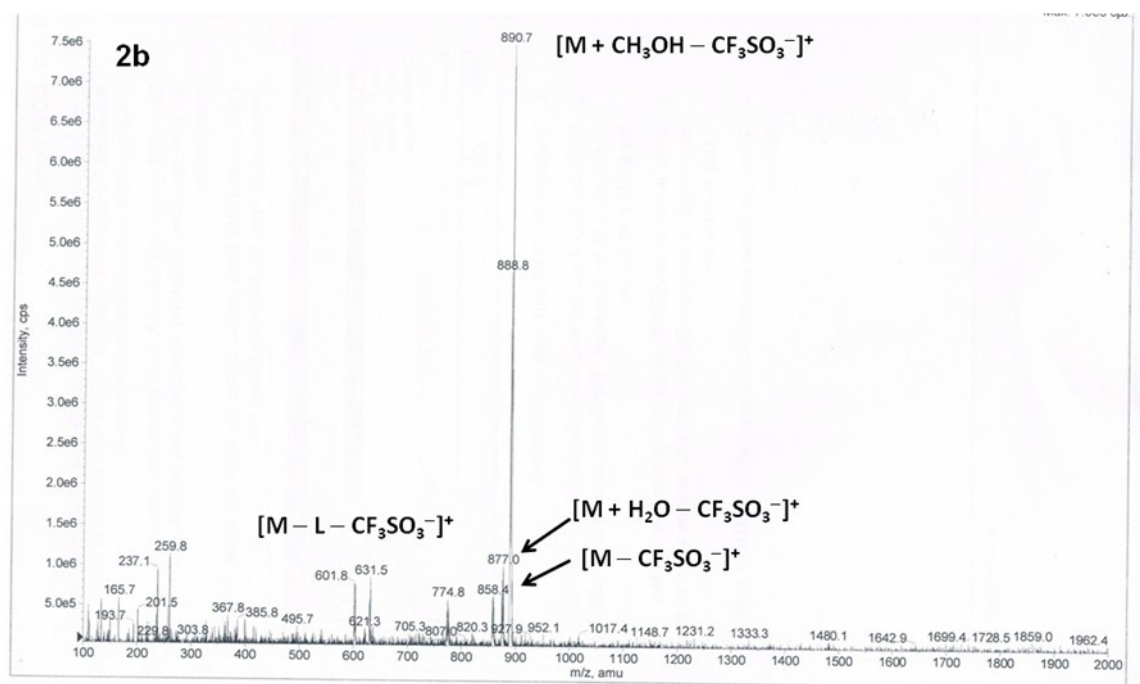


Fig. S6 ESI-mass spectrum of a mixture of complex **2c** (10 μ M) and NBO (10 mM) in methanol/water (1:1, v/v) at 298 K.

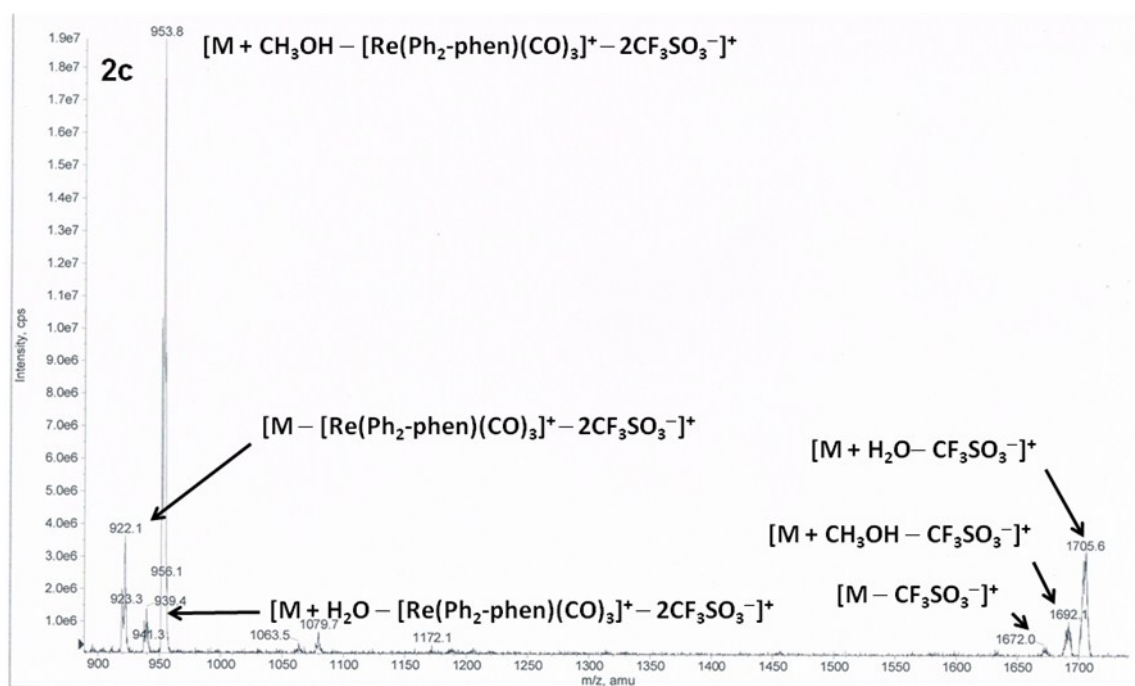


Fig. S7 ESI-mass spectrum of a mixture of py-3-Tz (10 μ M) and NBO (10 mM) in methanol/water (1:1, v/v) at 298 K.

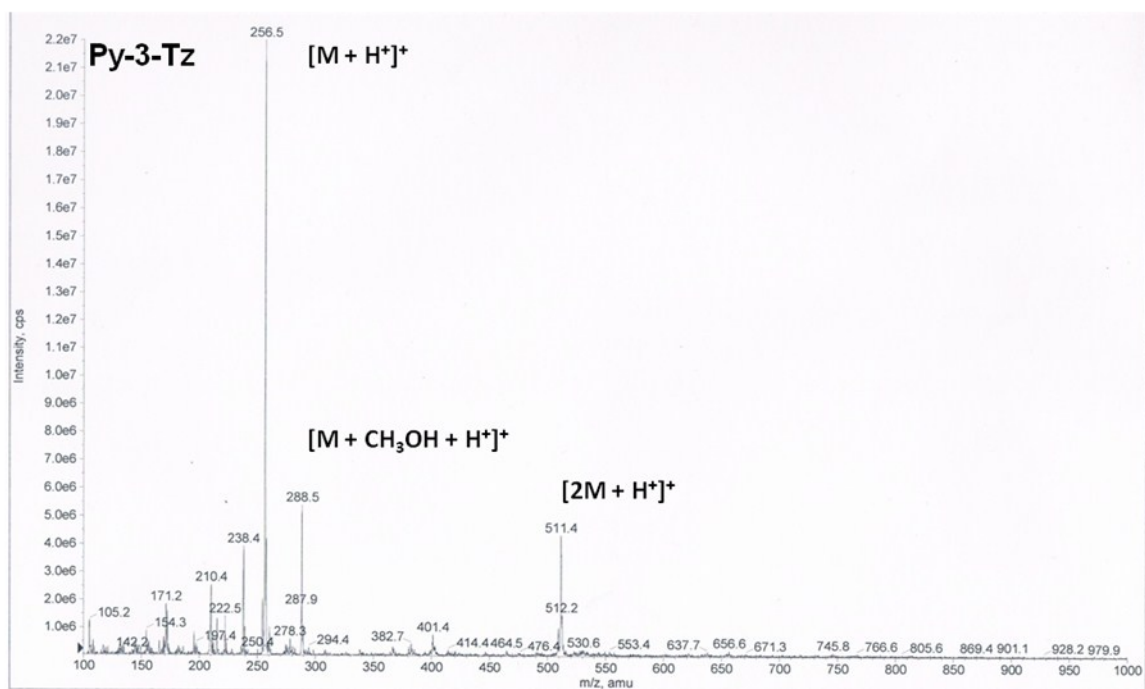


Fig. S8 ESI-mass spectrum of a mixture of py-4-Tz (10 μ M) and NBO (10 mM) in methanol/water (1:1, v/v) at 298 K.

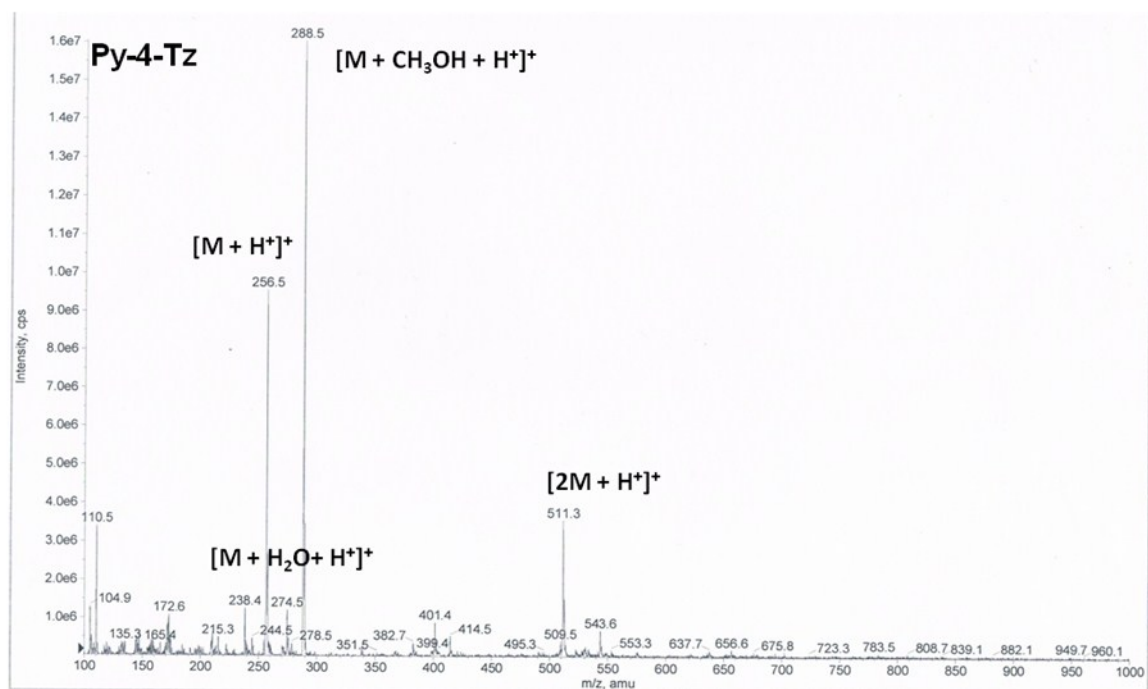


Fig. S9 ESI-mass spectrum of a mixture of py-Tz-py (10 μ M) and NBO (10 mM) in methanol/water (1:1, v/v) at 298 K.

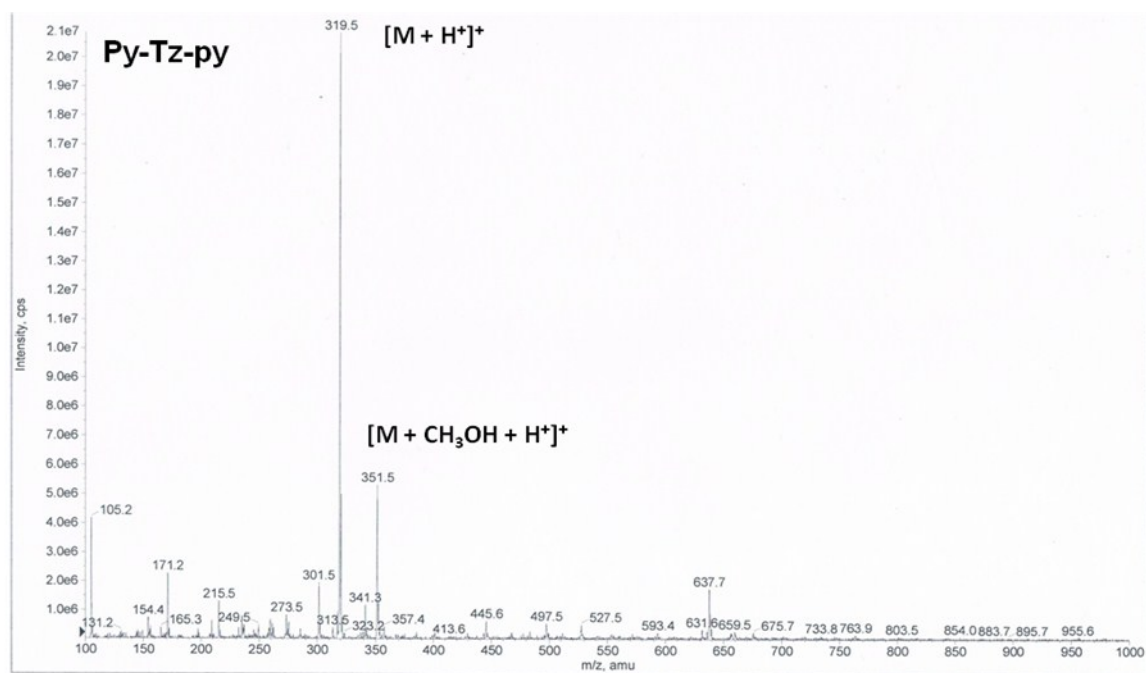


Fig. S10 ESI-mass spectrum of a mixture of complex **1a** (10 μM) and BCN (200 μM) in methanol/water (1:1, v/v) at 298 K.

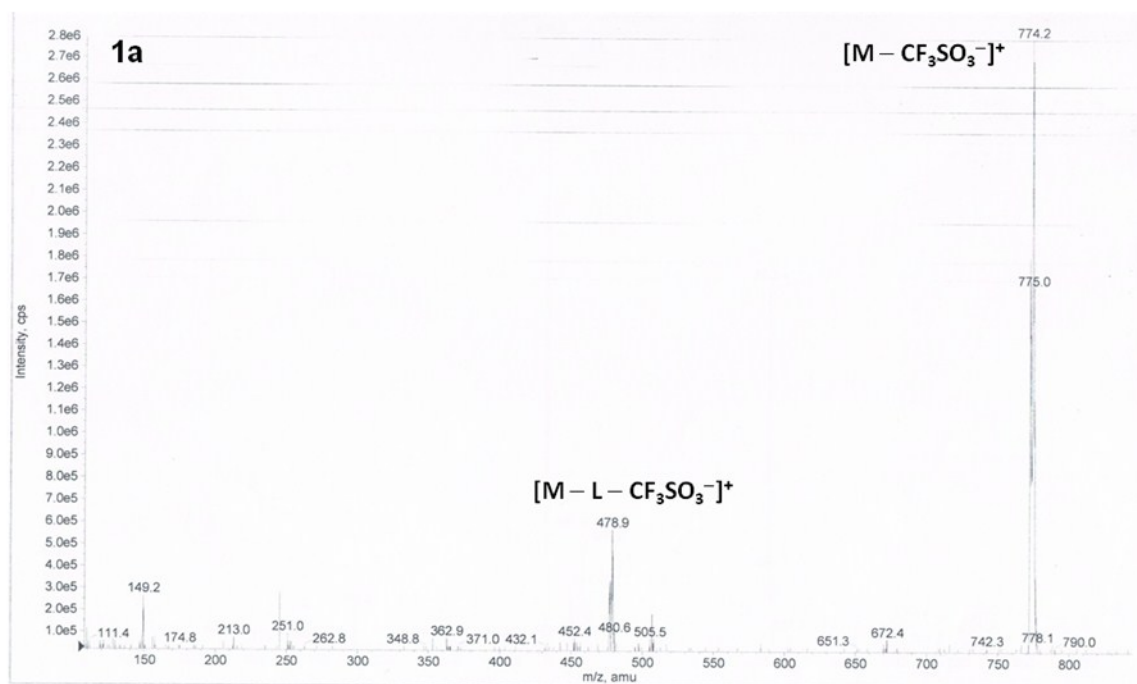


Fig. S11 ESI-mass spectrum of a mixture of complex **1b** (10 μM) and BCN (200 μM) in methanol/water (1:1, v/v) at 298 K.

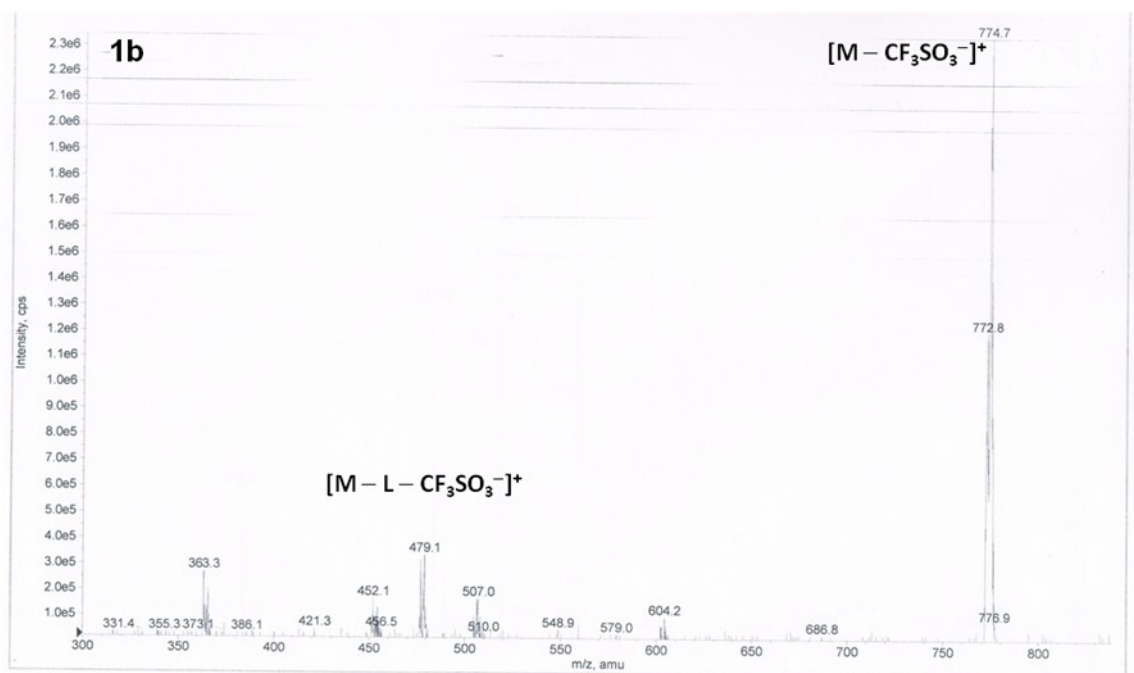


Fig. S12 ESI-mass spectrum of a mixture of complex **1c** (10 μM) and BCN (200 μM) in methanol/water (1:1, v/v) at 298 K.

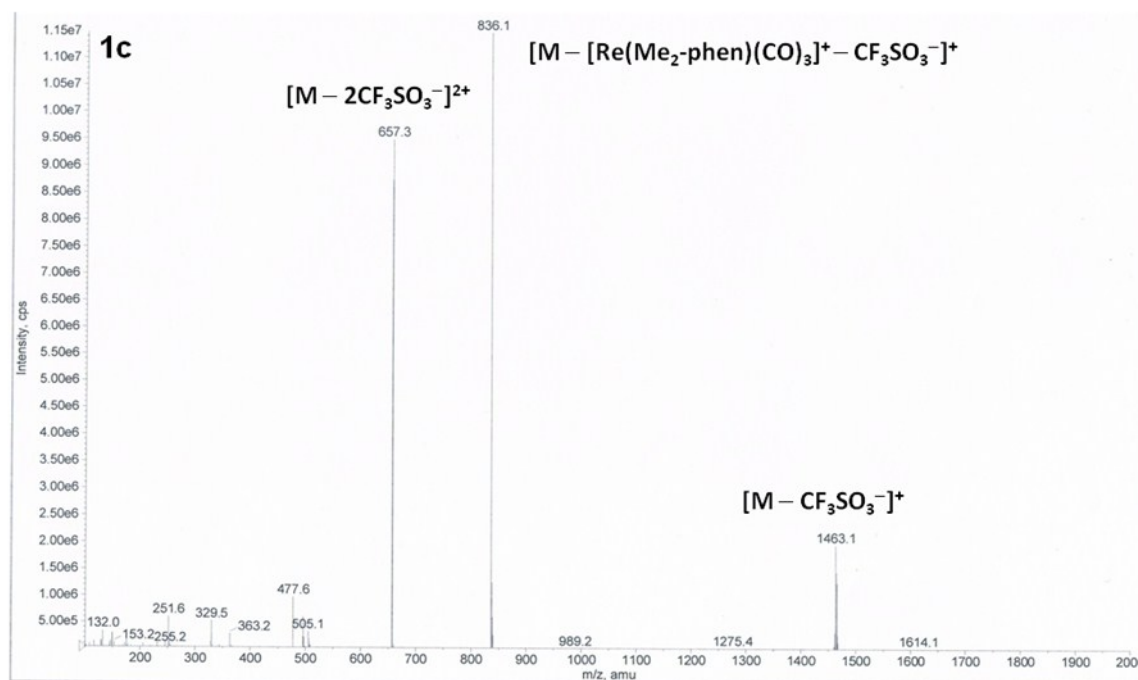


Fig. S13 ESI-mass spectrum of a mixture of complex **2a** (10 μM) and BCN (200 μM) in methanol/water (1:1, v/v) at 298 K.

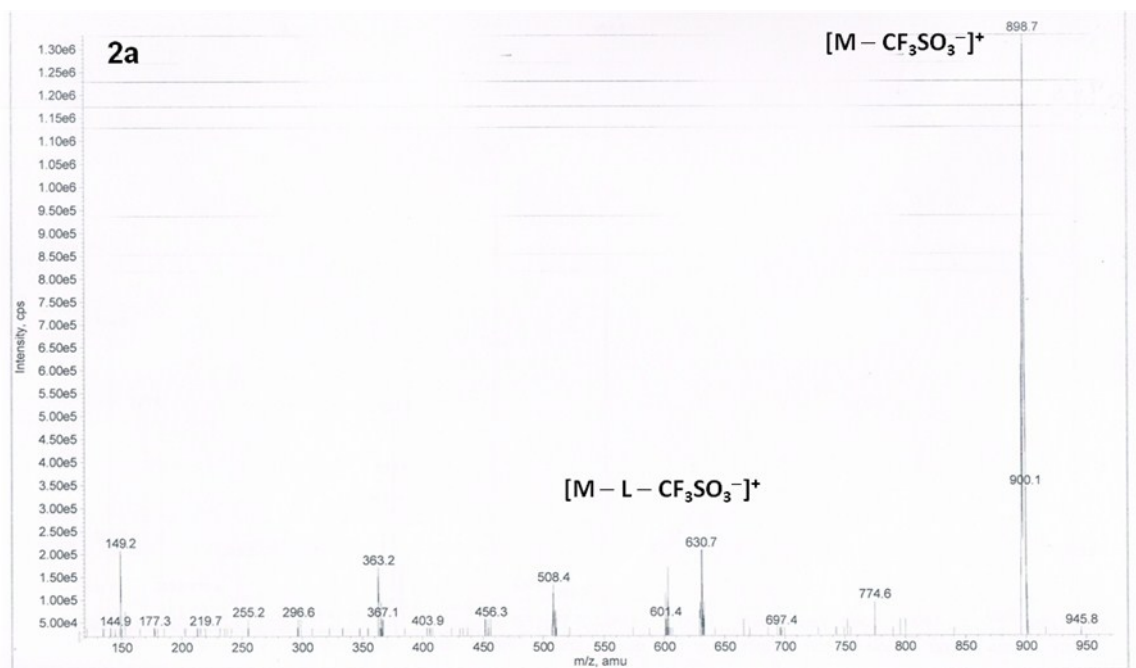


Fig. S14 ESI-mass spectrum of a mixture of complex **2b** (10 μM) and BCN (200 μM) in methanol/water (1:1, v/v) at 298 K.

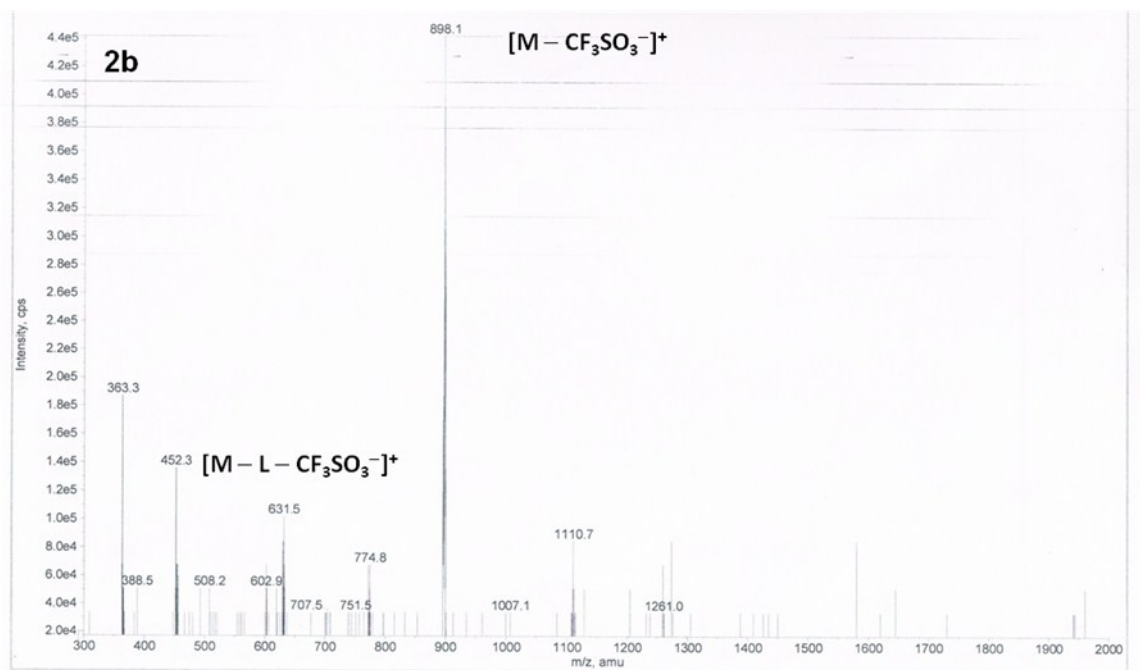


Fig. S15 ESI-mass spectrum of a mixture of complex **2c** (10 μM) and BCN (200 μM) in methanol/water (1:1, v/v) at 298 K.

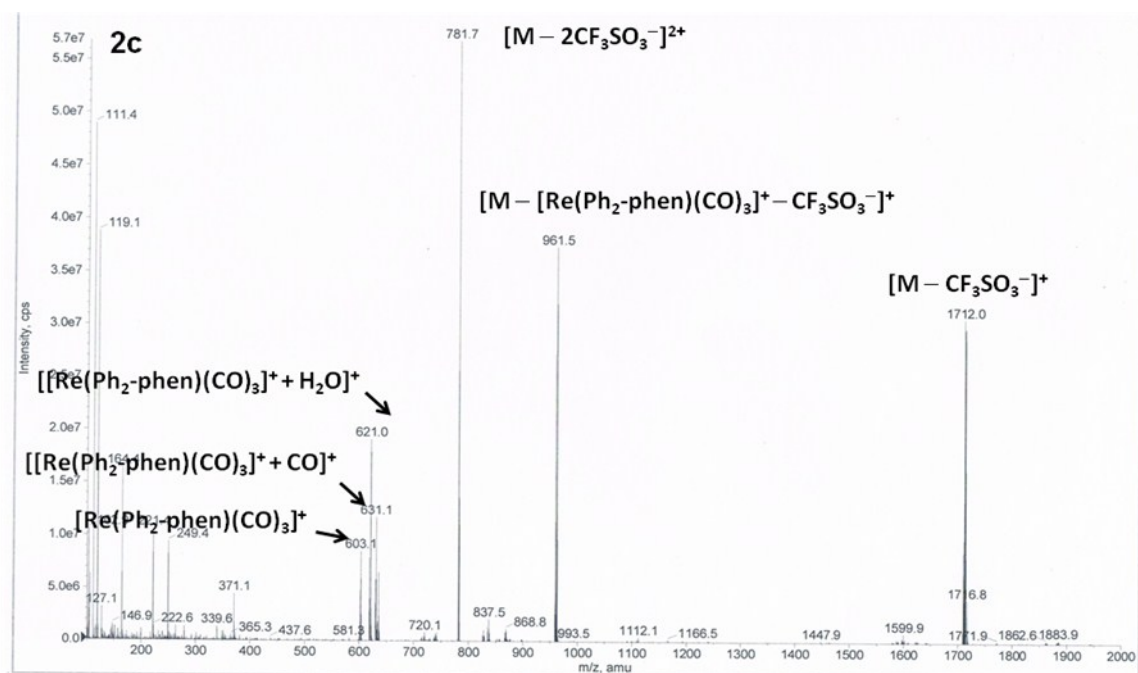


Fig. S16 ESI-mass spectrum of a mixture of py-3-Tz (10 μM) and BCN (200 μM) in methanol/water (1:1, v/v) at 298 K.

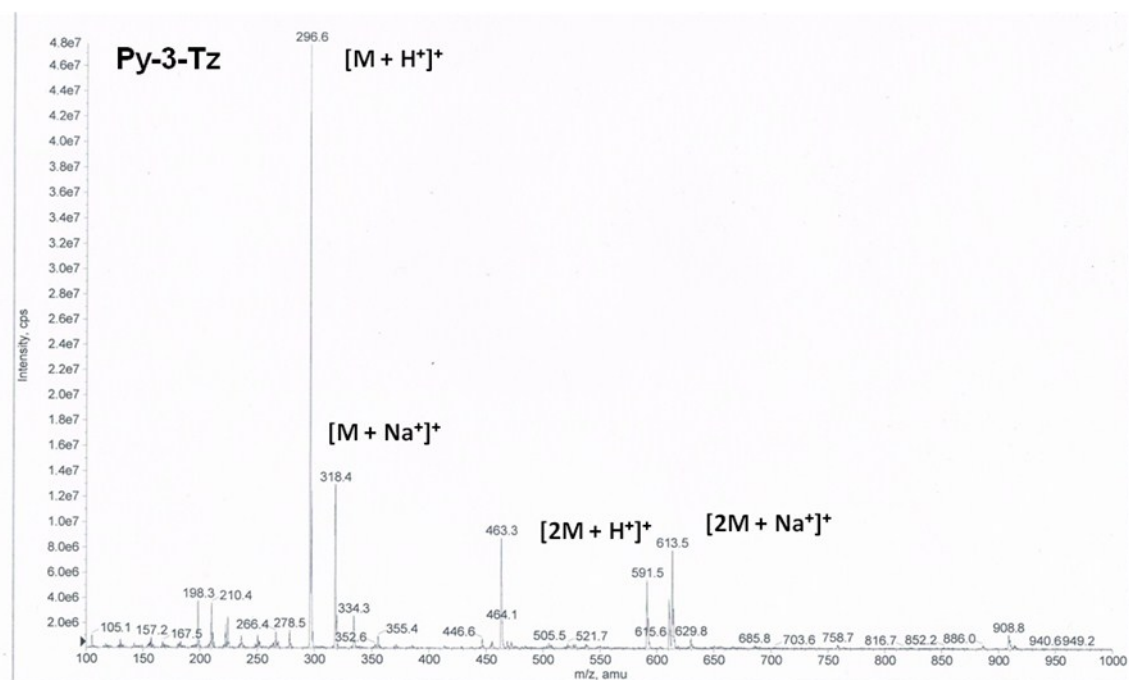


Fig. S17 ESI-mass spectrum of a mixture of py-4-Tz (10 μ M) and BCN (200 μ M) in methanol/water (1:1, v/v) at 298 K.

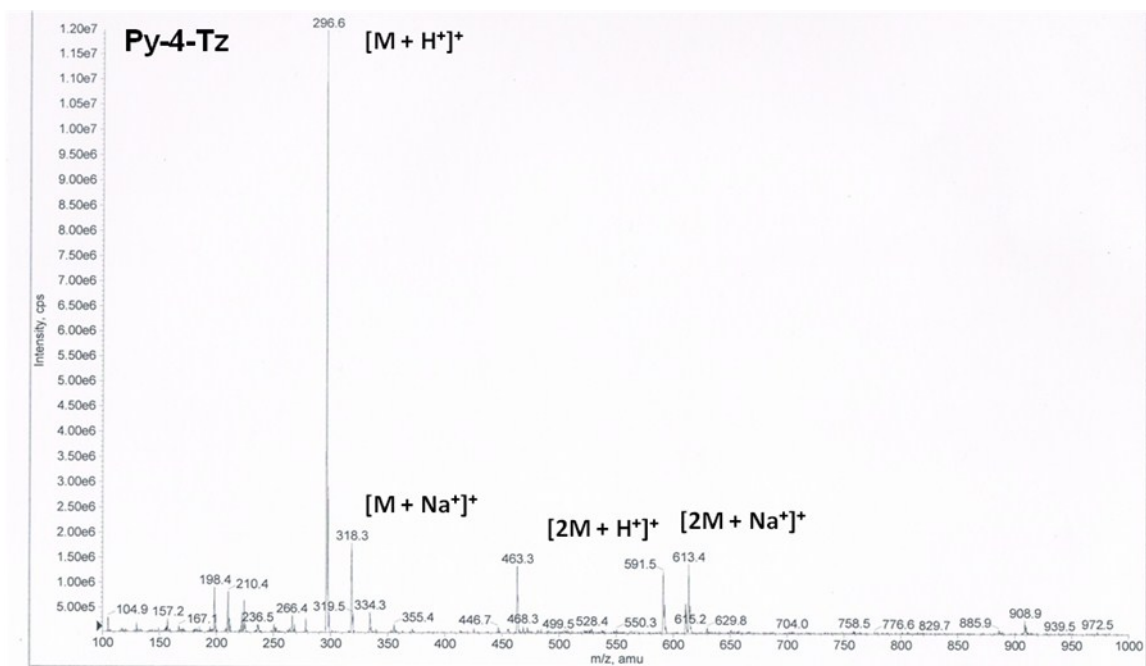


Fig. S18 ESI-mass spectrum of a mixture of py-Tz-py (10 μM) and BCN (200 μM) in methanol/water (1:1, v/v) at 298 K.

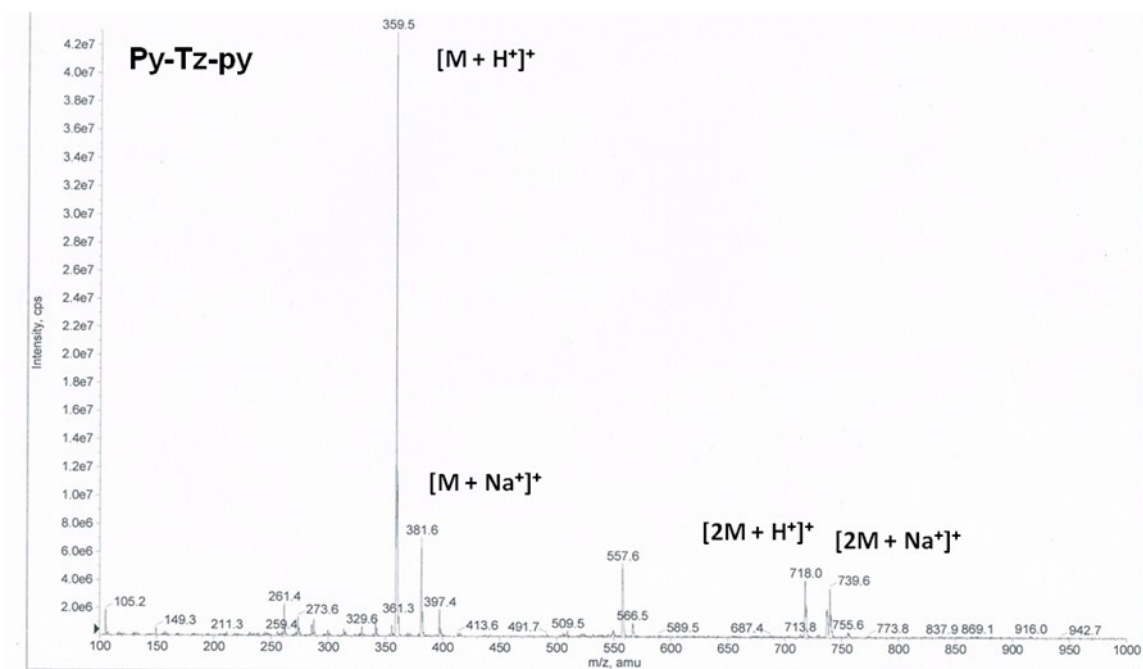


Fig. S19 Emission spectra of the tetrazine complexes (10 μM) in the presence of 0 (dashed) and 10 mM (solid) NBO, respectively, in methanol/water (1:1, v/v) at 298 K.

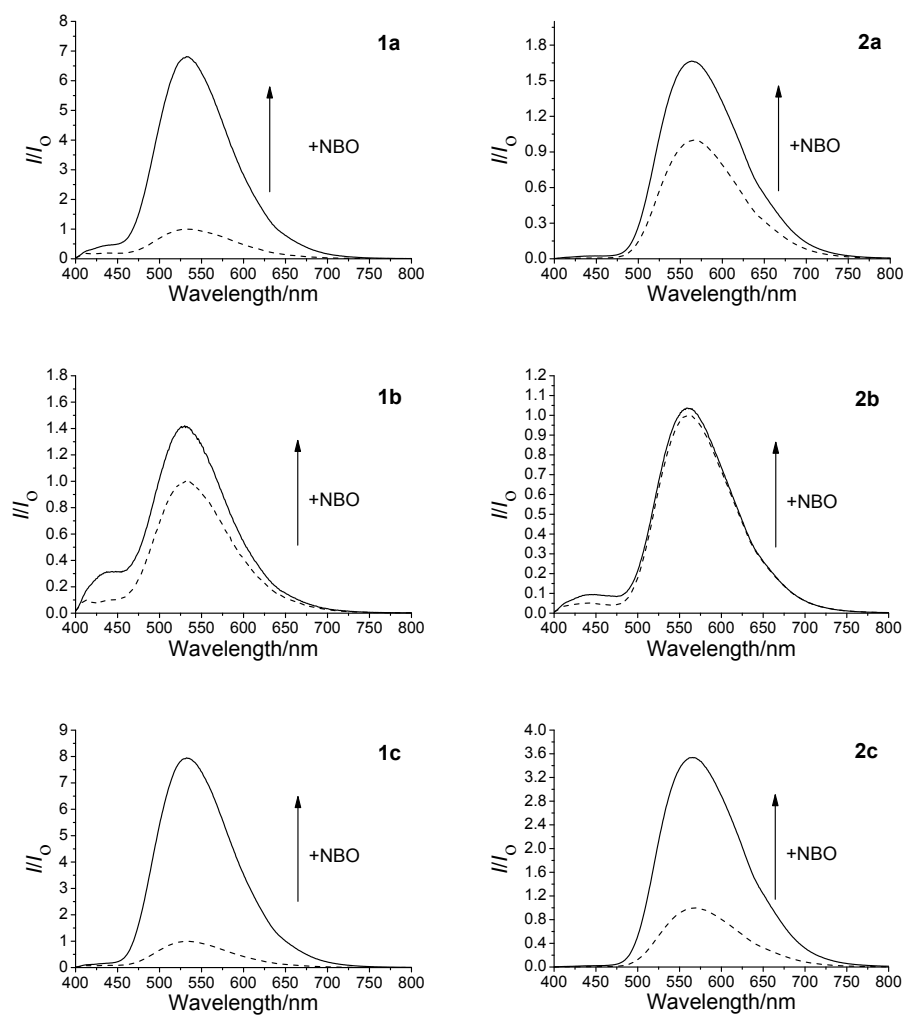


Fig. S20 Emission spectra of the tetrazine complexes (10 μM) in the presence of 0 (dashed) and 200 μM (solid) BCN, respectively, in methanol/water (1:1, v/v) at 298 K.

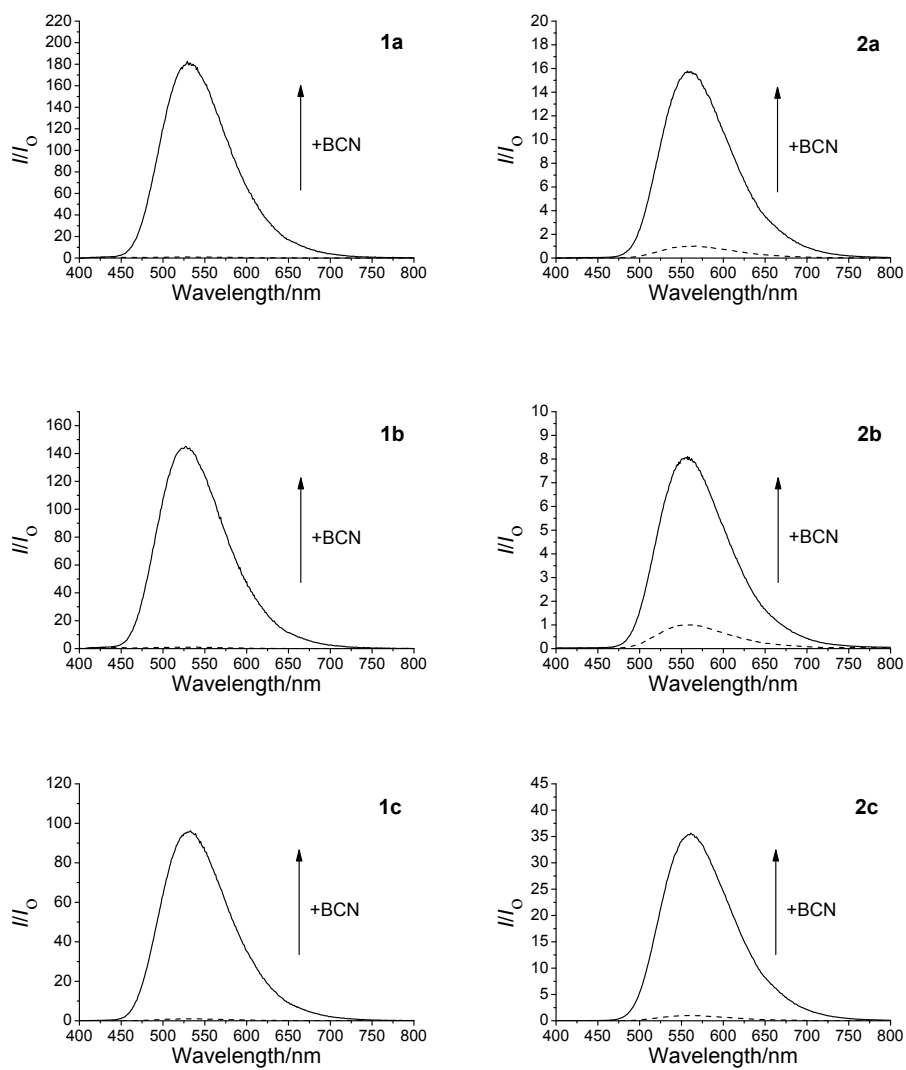
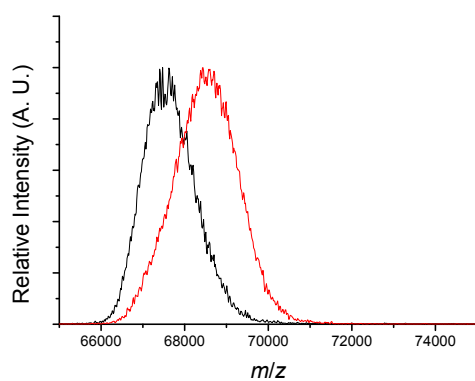
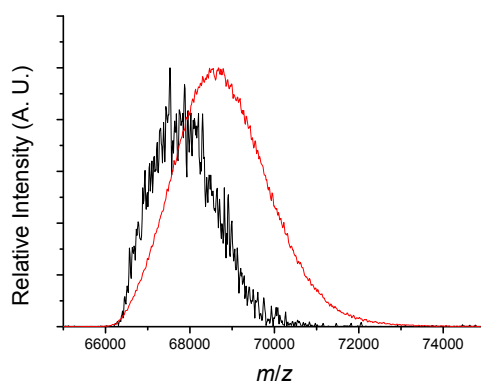


Fig. S21 MALDI-TOF-mass spectra of (a) unmodified BSA (black) and BSA-BCN (red), (b) unmodified HSA (black) and HSA-BCN (red) and (c) unmodified aTf (black) and aTf-BCN (red).

(a)



(b)



(c)

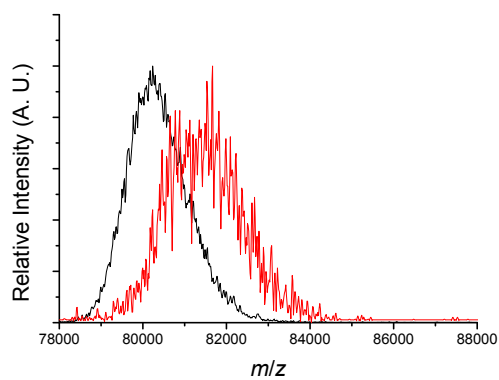


Fig. S22 SDS-PAGE analysis of BSA-BCN and unmodified BSA (7.4 μM) incubated with complexes **1a**, **1b** and **1c** (50 μM) for 1 h. Top: UV transillumination; bottom: Coomassie Blue staining. Lane 1: protein ladder; lane 2: unmodified BSA only; lanes 3, 5 and 7: BSA-BCN with complexes **1a**, **1b** and **1c**, respectively; lanes 4, 6 and 8: unmodified BSA with complexes **1a**, **1b** and **1c**, respectively.

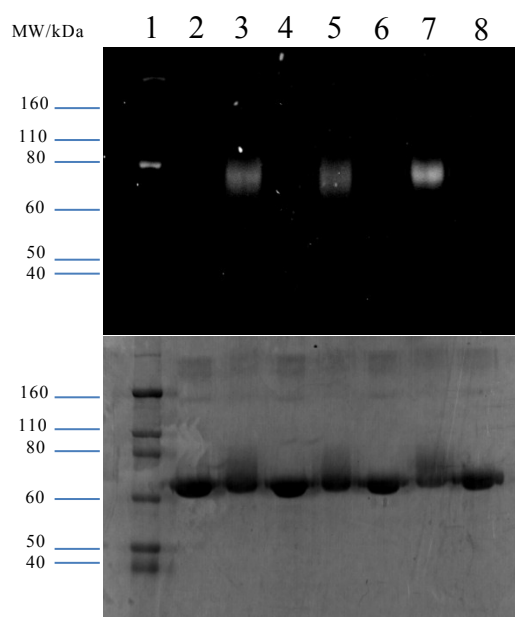


Fig. S23 SDS-PAGE analysis of BSA-BCN and unmodified BSA (7.4 μ M) incubated with complexes **2a**, **2b** and **2c** (50 μ M) for 1 h. Top: UV transillumination; bottom: Coomassie Blue staining. Lane 1: protein ladder; lane 2: unmodified BSA only; lanes 3, 5 and 7: BSA-BCN with complexes **2a**, **2b** and **2c**, respectively; lanes 4, 6 and 8: unmodified BSA with complexes **2a**, **2b** and **2c**, respectively.

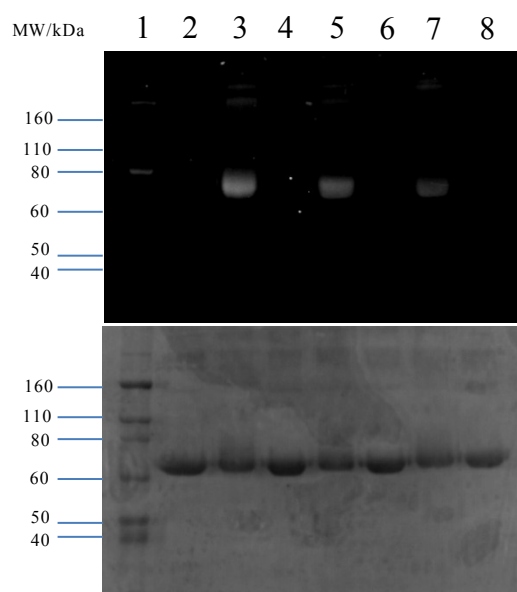


Fig. S24 MALDI-TOF mass spectra of unmodified BSA (black), BSA-BCN (red) and BSA-BCN labelled by complexes **1a** (blue), **1b** (magenta) and **1c** (green), respectively.

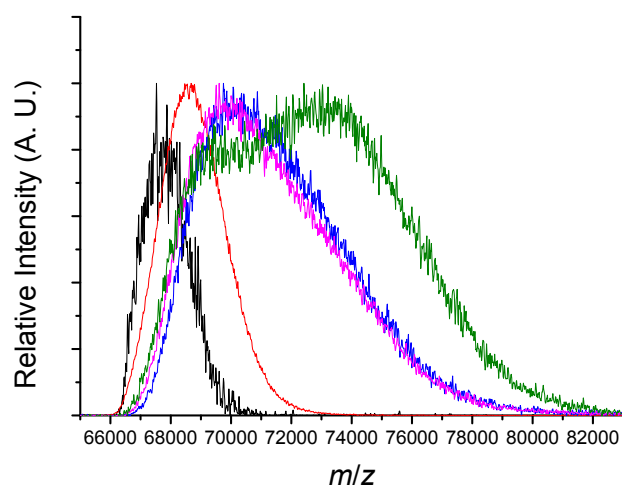
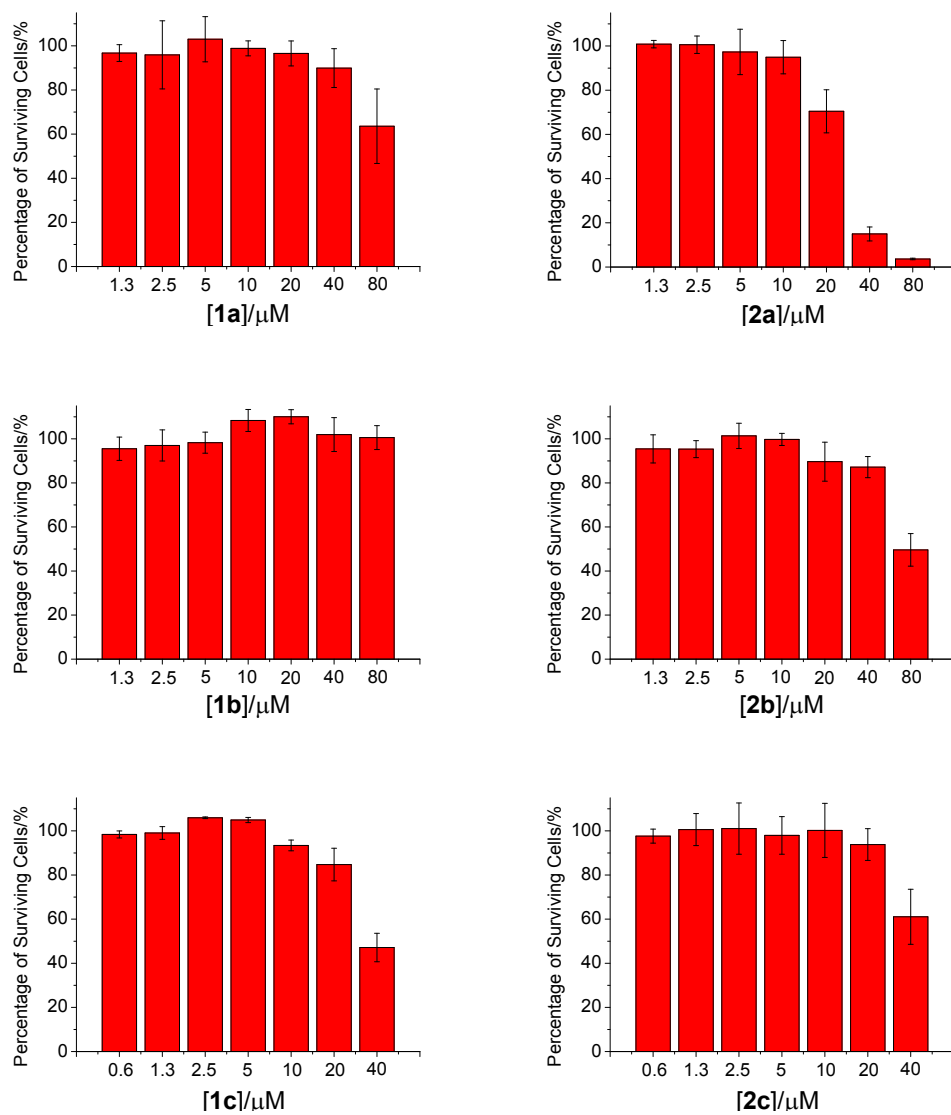


Fig. S25 Percentage of surviving HeLa cells after exposure to the tetrazine complexes at various concentrations at 37°C for 1 h.



References

- 1 D. D. Perrin and W. L. F. Armarego in *Purification of Laboratory Chemicals*, 3rd ed, Pergamon Press, New York, 1988.
- 2 K. K.-W. Lo and W.-K. Hui, *Inorg. Chem.* 2005, **44**, 1992.
- 3 J. N. Demas and G. A. Crosby, *J. Phys. Chem.* 1971, **75**, 991.
- 4 L. Wallace and D. P. Rillema, *Inorg. Chem.* 1993, **32**, 3836.
- 5 P.-K. Lee, H.-W. Liu, S.-M. Yiu, M.-W. Louie and K. K.-W. Lo, *Dalton Trans.* 2011, **40**, 2180.
- 6 M.-W. Louie, H.-W. Liu, M. H.-C. Lam, T.-C. Lau and K. K.-W. Lo, *Organometallics* 2009, **28**, 4297.